Available online at www.sciencedirect.com

ScienceDirect

Ceramics International 40 (2014) 5025–5031

CERAMICS INTERNATIONAL

www.elsevier.com/locate/ceramint

Short communication

Oxidation behavior of spark plasma sintered ZrC–SiC composites obtained from the polymer-derived ceramics route

David Pizon[a], Ludovic Charpentier[b], Romain Lucas[a,*], Sylvie Foucaud[a], Alexandre Maître[a], Marianne Balat-Pichelin[b]

[a]SPCTS-CNRS, UMR 7315, Centre Européen de la Céramique (CEC), 12 rue Atlantis, F-87068 Limoges Cedex, France
[b]PROMES-CNRS, UPR 8521, 7 rue du four solaire, F-66120 Font-Romeu Odeillo, France

Received 19 March 2013; received in revised form 25 August 2013; accepted 26 August 2013
Available online 5 September 2013

Abstract

ZrC_m/SiC_p composites were elaborated using the polymer derived ceramics route and the spark plasma sintering process. The results of mechanical and microstructural characterization of composites were undertaken, and indicated an improvement by adding the SiC phase. The oxidation resistance of composites was evaluated at very high temperatures, and a better behavior was observed whatever the SiC content compared to ZrC monoliths. By adjusting the composition of the final composite, two main ranges of stability were determined as a function of the heat treatment.

Keywords: ZrC; SiC; Particular composites; Polymer processing; Oxidation resistance

1. Introduction

Ultra-High Temperature Ceramics (UHTCs) based on the carbides, nitrides and borides of the groups 4 and 5 transition metals have received considerable attention, due to their unique combination of properties, such as melting temperature above 2000 K, hardness, high electrical and thermal conductivities, as well as chemical inertness against molten metals. UHTCs represent a class of promising materials for use in high temperature applications, such as sharp leading edges on future generations of reentry vehicles, solar receivers of concentration solar power plants, cladding of the nuclear fuel for the future 4th generation systems, elements of combustion chambers and so on. ZrC has been given special attention because of its melting point around 3500 K, relatively low density, good strength at high temperatures, and high elastic modulus [1].

Oxidation resistance is a critical aspect in the development of UHTCs. Indeed, ZrC has a poor high-temperature chemical stability in an oxidizing atmosphere, which significantly limits its actual application as UHTCs. A common approach to improve the oxidation resistance of ZrC is the incorporation of Si-containing compounds into UHTCs matrix to form a protective SiO_2-containing oxide scale. Such behavior requires a homogenous microstructure in terms of chemical composition and grain size distribution. The MC/SiC (where M = Ti, Zr, Hf) composites were usually done by sintering of carbide powders, microwave activation and polymer impregnation pyrolysis [2–4]. However, these studies show it is difficult to obtain homogeneous materials. In this case, the Polymer-Derived Ceramics (PDCs) route seems to be promising [5–8]. Indeed, this method could be suitable to obtain a hybrid material in which a mineral ZrC powder could be coated by the precursor, and could lead to a composite with a homogeneous microstructure after pyrolysis [9–12]. In addition, fully dense composites without sintering additives have hardly been obtained because of high melting temperature and strong covalent bonding of ZrB_2, SiC and ZrC [13,14]. Besides, Spark Plasma Sintering (SPS) allows the densification of ZrB_2/ZrC/SiC composites at a lower temperature and in a shorter time compared with conventional techniques [13,15,16]. So, the combination of PDCs and SPS could be a promising way to reach oxidation-resistant composites in the Zr–Si–C system.

*Corresponding author. Tel.: +33 587 502 350; fax: +33587502304.
E-mail address: romain.lucas@unilim.fr (R. Lucas).

0272-8842/$ - see front matter © 2013 Elsevier Ltd and Techna Group S.r.l. All rights reserved.
http://dx.doi.org/10.1016/j.ceramint.2013.08.105

In this study, ZrC_m/SiC_p composites were shaped and sintered by coupling the PDCs and SPS methods with different compositions, microstructures and mechanical properties. The reactivity of these composites in air at high temperature was also evaluated.

2. Experimental

2.1. Materials

The ZrC powders were purchased from Alfa Aesar (99.5%). The polycarbomethylsilane (PCMS) (Aldrich, 99.9%, $M_w \approx 800\ g\ mol^{-1}$) adopts the molecular formula $(C_2H_6Si)_n$. It is a white solid with a melting point of around 357 K. This polymer was used as received.

2.2. Composites preparation

The samples of the ZrC_m/SiC_p composites were elaborated with 10 and 30 wt% SiC (compositions **2** and **3**, Table 1). The first step consists in a crosslink of the PCMS in air atmosphere during 10 h at 523 K. The crosslinked polymer was mixed with ZrC powders. Afterwards, the mixture was pyrolyzed in argon at 873 K for 5 h. The residue so-obtained was then ball milled (planetary mono mill, Fritsch, Germany). ZrC/SiC composites were sintered by using a SPS apparatus (Syntex, Dr. Sinter 825, Japan) at 2223 K for 15 min in vacuum, with heating rates of 100 K/min up to 2173 K, then of 50 K/min up to 2223 K. A uniaxial pressure of 50 MPa was applied during the heat treatment. For the composition **1**, ZrC was directly sintered by SPS without previous treatment and using the same conditions described above.

2.3. Characterization

Considering the SPS sintered samples, their final densities were determined using the Archimedes method. Apparent elastic constant (Young's modulus) has been obtained thanks to the ultrasonic method using 10 MHz transducers working in reflexion mode (WC37-10 and SW37-10, Ultran, State College, USA) on 5 mm thick samples [17]. Phase identification was carried out by X-ray diffraction, using a device type Siemens D5000 (2θ, Cu K_α) (Germany) and Scanning Electron Microscopy (XL30 PhilipsTM, Eindhoven, Netherlands) coupling with an Energy Dispersive X-ray Spectroscopy (EDXS) device.

Table 1
Mass fraction of different phases, relative density, and Young's modulus values for ZrC–SiC composites.

Sample composition	Mass fraction (wt%)		Relative density (%)	Young's modulus (GPa)
	ZrC	SiC		
1	100	0	87	252 ± 2
2	90	10	100	410 ± 2
3	70	30	97	424 ± 2

2.4. Oxidation tests

The oxidation tests were performed using the REHPTS (REacteur Hautes Pression et Température Solaire) facility implemented at the focus of the 5 kW Odeillo solar furnace [18]. Samples were placed 25 mm above the focus, a shutter located between the concentrator and the reactor enables to control the fraction of the concentrated solar flux transmitted to the sample. The sample is irradiated on all its surface by the solar radiation with an homogeneous zone of 10 mm in the center. The temperature is measured at the center of the sample – on a 6 mm diameter circle – using a monochromatic (5 μm) optical pyrometer IRCON and the temperature level can be adjusted by playing on the opening of the shutter. The normal spectral emissivity used to obtain the real temperature by monochromatic pyrometry is measured on another experimental set-up in our lab [19–21]. For these experiments, the sample at the beginning of oxidation is immediately covered by an oxide layer mainly composed of zirconia and the value taken for its emissivity at 5 μm is 0.75. The reactor is open to the surrounding air at a total pressure of 87 kPa (due to the fact the set-up is located at PROMES laboratory in Odeillo, 1500 m above the sea level). Such a set-up enables fast heating of the samples (with rates up to $100\ K\ s^{-1}$), and the samples were maintained during 20 min at the desired temperature plateau during oxidation. Each experiment was filmed using a video camera, and the mass variation rate was determined by weighing the sample before and after experiment, then by reporting the mass variation to the initial surface and the duration of the temperature plateau, in order to obtain a rate expressed in $mg\ cm^{-2}\ min^{-1}$. A global average oxidation rate (during 20 min) will be used during the future discussions.

3. Results and discussion

The three considered materials were sintered by SPS technique (Table 1). Concerning the composition **1**, a low relative density was obtained, explaining the low Young's modulus measured (252 GPa). Indeed, the commercial ZrC powders present a high grain size (average diameter of 8.6 μm), and so it is difficult to reach the theoretical density of ZrC without sintering additives, even with the SPS method. For the compositions **2** and **3**, two phases were identified: β-SiC and ZrC (Fig. 1 (a–d)). The micrographs indicate that the distribution of the two phases is globally homogeneous at the scale of the SEM technique. However, several aggregates were identified for composites **2** (Fig. 1 (b) and (d)). No microcrack was observed, and ZrC grains (gray) indicate an average size between 5 and 10 μm, while SiC elementary grains (in black) have diameters below one micrometer. In addition, richer silicon carbide areas were obtained for the composition **3** (Fig. 1 (b)).

The presence of these two phases is in agreement with previous results on composites synthesized from the polymer-derived ceramics route [11]. Furthermore, thanks to TEM observations (Fig. 1 (e)), graphite was highlighted as inclusions in the microstructure. This carbon phase could notably

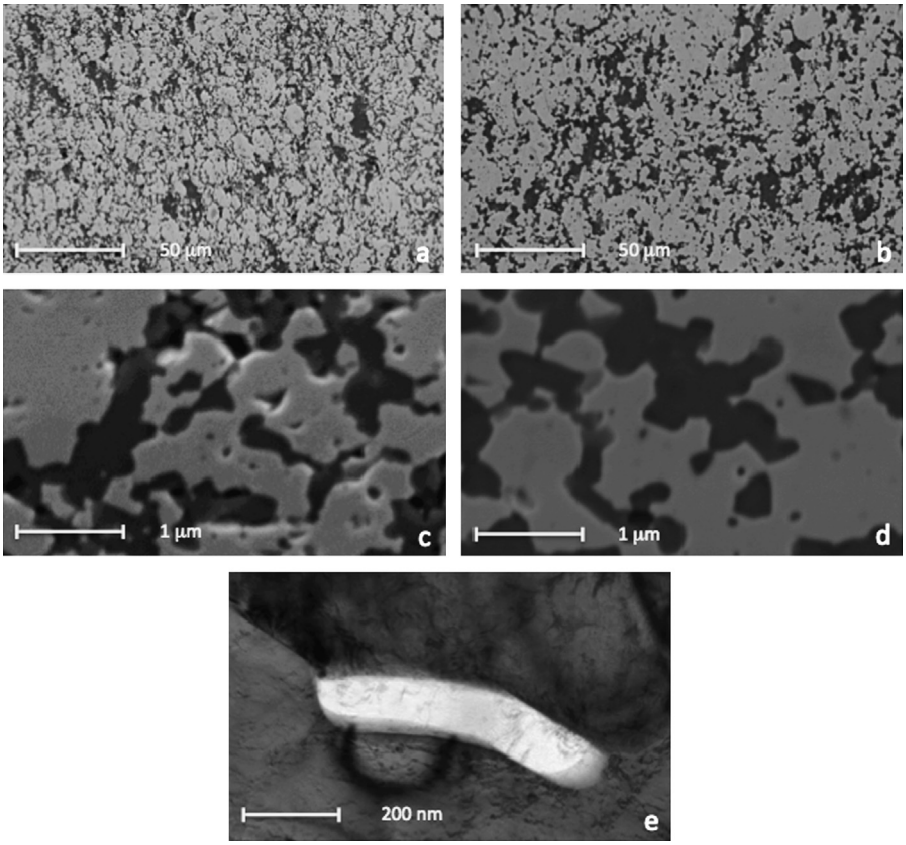

Fig. 1. SEM micrographs of sintered materials **2** (a) and (c), **3** (b) and (d); gray: ZrC, black: β-SiC; and TEM micrograph of the sample **2** (e) indicating a carbon inclusion (white).

stem from the pyrolyzed PCMS remnants. A higher value of the relative density is reached when the amount of SiC is slightly lower as indicated in Table 1: the precursor of the β-SiC phase would seem to promote the densification rate of ZrC-based composites. In the same way, the Young's modulus were enhanced by introducing β-SiC particles, in comparison with the Young's modulus values of dense ZrC material around 390–400 GPa, reported in the literature [22]. Therefore, using the SPS protocol described before, the intrinsic properties of the ZrC monoliths obtained from micrometric powders, in terms of density and Young's modulus, were increased by synthesizing ZrC/SiC composites.

Since these materials would be used under severe conditions like high temperature and oxidative atmosphere, a study of the mass variation of the different samples was then carried out (Fig. 2).

The three kinds of samples were oxidized in ambient air to give $\mathbf{1}_{ox}$, $\mathbf{2}_{ox}$, and $\mathbf{3}_{ox}$. Each point represented in Fig. 2 corresponds to a new sample used for each temperature level. It was difficult to reach higher temperature level than 1830 K with pure ZrC samples due to the growth of one white and insulating pure layer of ZrO_2. This modification of surface composition implies difficulty in controlling the temperature plateau and a variation up to $\pm$ 50 K is observed. Zirconium carbide (**1**), as a reference, indicated a mass gain rate of around 4 mg cm^{-2} min^{-1} between 1350 and 1450 K, followed by a decrease up to 2.61 mg cm^{-2} min^{-1} at 1840 K.

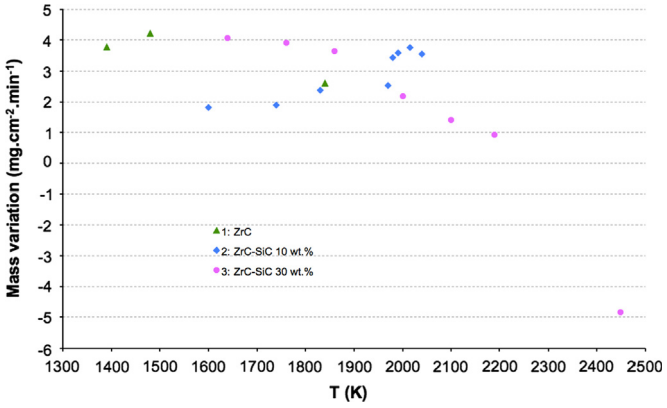

Fig. 2. Mass variation rate as a function of temperature, during the oxidation of compositions **1**, **2** and **3**.

The conversion of ZrC to ZrO_2 at the specimen surface can explain these results. Indeed, zirconium carbide is known to be oxidized from 1000 K in air [23]. Thus, a first weight gain is observed which can be justified by the formation of solid zirconia, and carbon according to Eq. (1). Afterwards, the release of carbon dioxide could explain the lower mass variation rate (Eq. (2)). Concerning the composites **2** and **3**, a first mass gain was observed up to 1800 K. This tendency is due to the surface nucleation of solid oxides according to Eqs. (1)-(3). However, above 1800 K, the

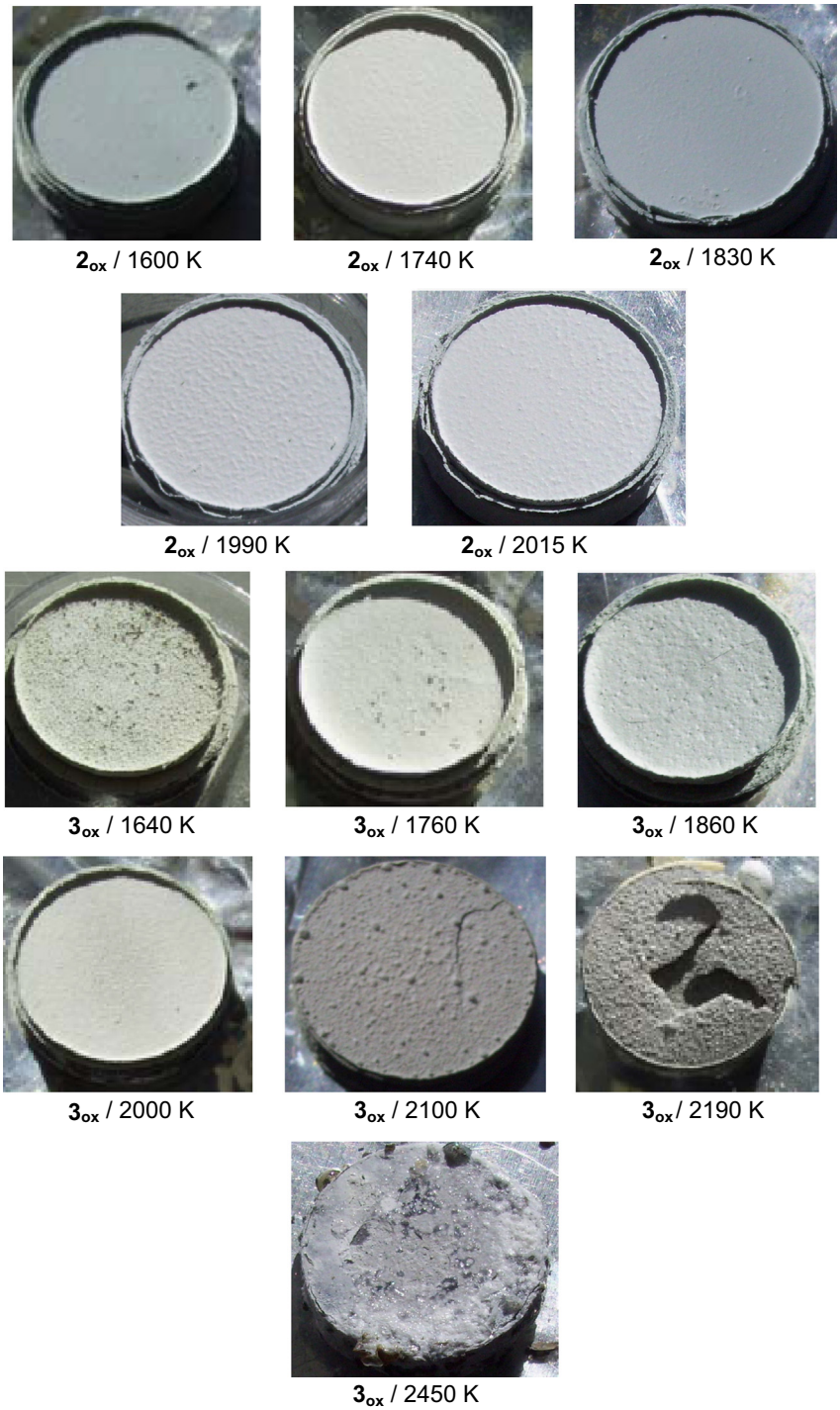

Fig. 3. Pictures of the oxidized samples for the two compositions **2** (ZrC–10%SiC) and **3** (ZrC–30%SiC).

composite **2** shows a mass gain up to 2000 K, while the composite **3** presents a decreasing mass gain. The composite is even losing some mass at 2450 K. The addition of 10 wt% SiC leads to a mass gain increase from 1600 K up to 2015 K. This phenomenon can be related to the formation of a zirconia enriched oxide layer. Conversely, the addition of 30 wt% SiC leads to a continuous decrease of the mass gain from 1640 K to 2190 K, and then is much more important at 2450 K. When the temperature ranges between 1950 and 2000 K, the mass loss rate can be correlated to the active oxidation of SiC, which rests on the removing of volatile phases as reported in Eq. (4). At the highest temperature (i.e. 2450 K), a higher mass loss rate ($\approx 5\ \mathrm{mg\ cm^{-2}\ min^{-1}}$) is recorded. This observation could be related to both the silicon carbide active oxidation and mainly to the SiC dissociation and

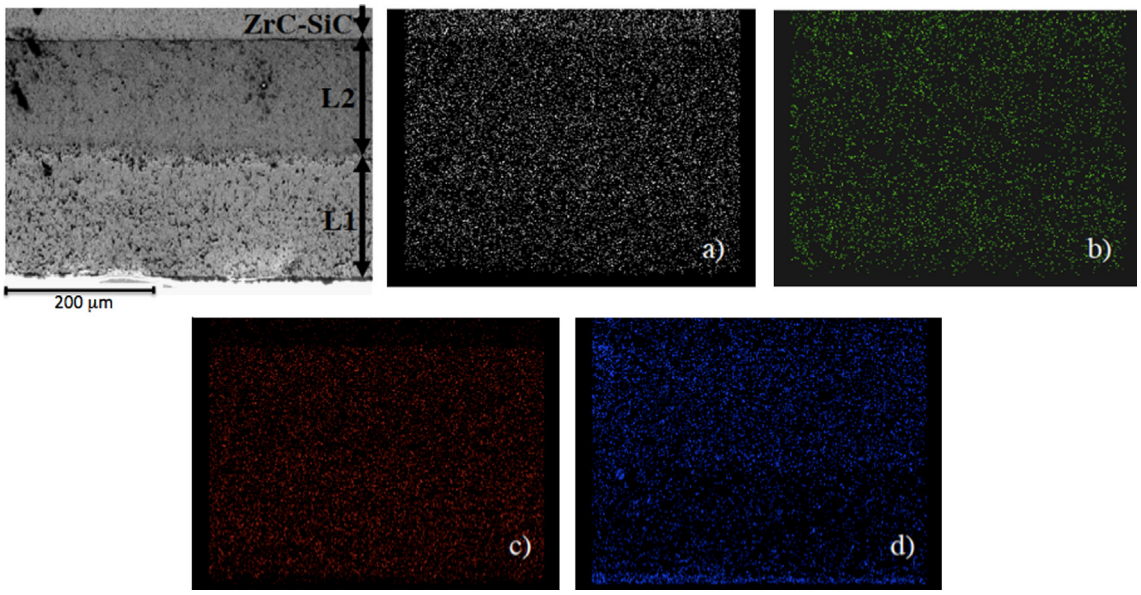

Fig. 4. SEM micrograph of the cross-section of the oxidized composite **2**$_{ox}$ at 2000 K, and EDXS cartography: zirconium (a), silicon (b), oxygen (c), and carbon (d).

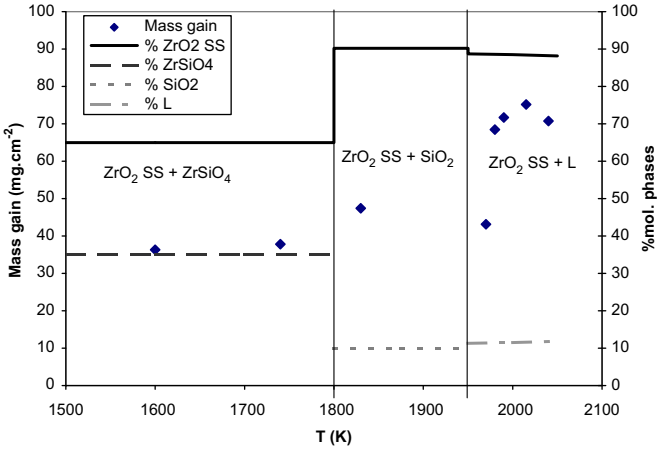

Fig. 5. Comparison between the measured mass gain and the phase proportions from the phase diagram for the system ZrO_2–SiO_2 extracted from [26], ZrC/10 wt% SiC.

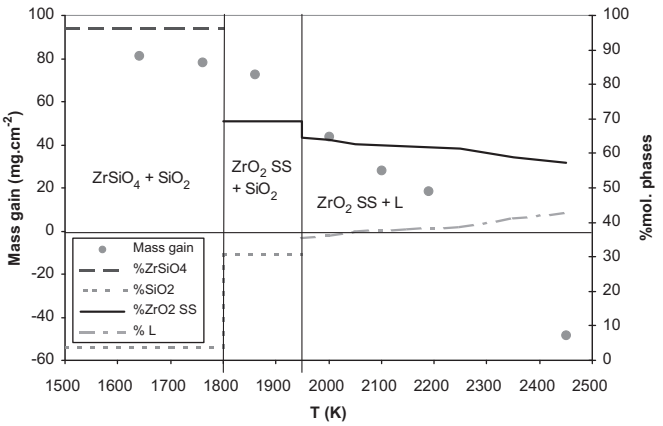

Fig. 6. Comparison between the measured mass gain and the phase proportions from the phase diagram for the system ZrO_2–SiO_2 extracted from [26], ZrC/30 wt% SiC.

sublimation according to Eqs. (5–7) (leading to silicon, SiC_2 and Si_2C), that are the predominant reactions in this temperature range [24].

$$ZrC_{(s)} + O_{2(g)} = ZrO_{2(s)} + C_{(s)} \quad (1)$$

$$ZrC_{(s)} + 2O_{2(g)} = ZrO_{2(s)} + CO_{2(g)} \quad (2)$$

$$SiC_{(s)} + 3/2O_{2(g)} = SiO_{2(s)} + CO_{(g)} \quad (3)$$

$$SiC_{(s)} + O_{2(g)} = SiO_{(g)} + CO_{(g)} \quad (4)$$

$$SiC_{(s)} = Si_{(g)} + C_{(s)} \quad (5)$$

$$2SiC_{(s)} = Si_{(g)} + SiC_{2(g)} \quad (6)$$

$$2SiC_{(s)} = C_{(s)} + Si_2C_{(g)} \quad (7)$$

The oxidized samples (Fig. 3) have been observed by means of optical microscopy. First, the treated surface of **2**$_{ox}$ remains smooth without macroscopic defects up to 1740 K. Above 1800 K, the oxide layer seems to come off the surface of the composite. Despite this phenomenon, which should be characteristic of the gas release, no morphological variation has been observed. For the composite **3**$_{ox}$, below 2000 K, the same phenomena have been identified for the **2**$_{ox}$ sample. But above 2100 K, the oxide layer presents some cracks and even macro-porosities appear after heating at 2450 K.

To focus on the effect of high-temperature oxidation on the microstructure of the composite, Fig. 4 shows the cross-section micrograph of the oxide layers of the sample of type **2**$_{ox}$, after oxidation at 2000 K. An EDXS cartography was carried out on the oxygen element to investigate the mechanism. The oxide-phase coating is clearly composed of two layers [L1+L2], with a thickness of 230 µm each. According to complementary

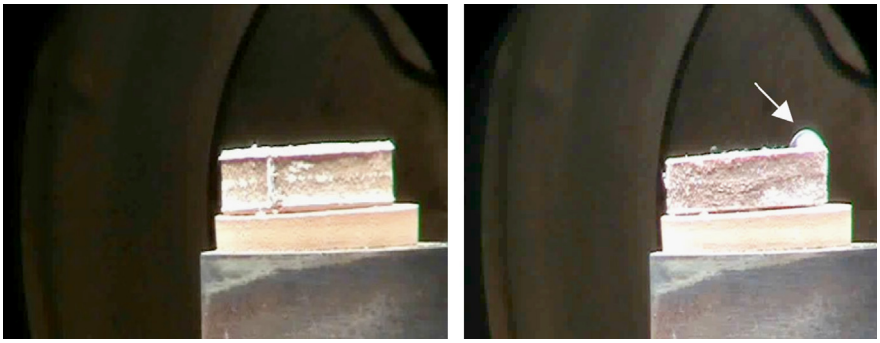

Fig. 7. Images of the oxidation of the composites **2** (T=2000 K, left) and **3** (T=2000 K, right) after 15 min oxidation. The white arrow indicates the presence of one bubble. For the videos, please refer to the annex.

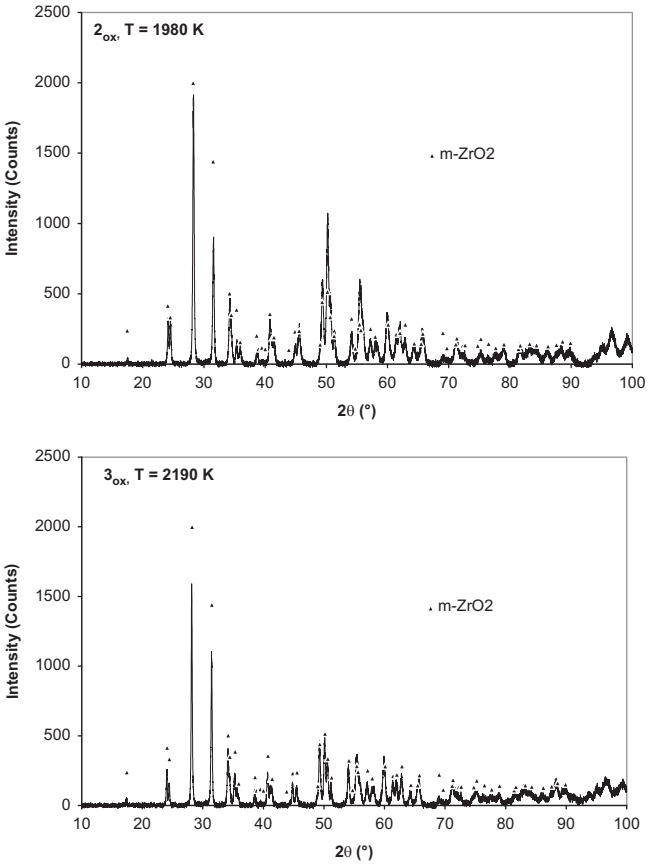

Fig. 8. XRD patterns of the composites $\mathbf{2_{ox}}$ and $\mathbf{3_{ox}}$ after oxidation.

EDXS analyses, the layer L2 would be ZrO_2, SiO_2 and residual carbon, and the external layer L1 would be composed only of ZrO_2 and SiO_2. The presence of free carbon only in a layer close to the interface was also reported by Shimada [23]. This latter author explained the growth of zirconia by a two step process, with first the formation of a transient zirconium oxycarbide $ZrO_{2-x}C_x$ then followed by the complete oxidation into ZrO_2.

Figs. 5 and 6 compare, in the conditions of thermodynamic equilibrium, the evolution of the mass variation and the expected amount of phases according to the temperature for ZrC/10 wt% SiC and 30 wt% SiC, respectively. The oxide layer, which grows on ZrC/10 wt% SiC surface should be composed of zirconia and zircon up to 1800 K, whereas ZrC/30 wt% SiC surface should be made of silica and zircon up to 1800 K. Then above 1800 K zircon may decompose into zirconia and silica. Above 1950 K a SiO_2 enriched liquid phase could appear on both materials. The different behavior seems to be due to a higher content of this silica-based oxide that could form for the ZrC/30 wt% SiC, this content increasing with temperature. This liquid phase may favor the release of gaseous compounds such as CO and SiO through boiling [25]. ZrC/10 wt% SiC would form an oxide layer richer in zirconia with a very low content in silica, therefore its oxidation kinetics may only increase with temperature as zirconia is not supposed to volatilize, contrary to silica.

Fig. 7 presents the video captions of the experiments after 15 min at 2000 K. The formation of bubbles was displayed during the oxidation of the composite **3**, in agreement with the production of a more important amount of liquid phase and/or of gaseous products due to the higher content of SiC in the composite, as shown on Figs. 5 and 6. At the same time, the composite **2** exhibits less surface deformation, evidencing the formation of less liquid phase and/or fewer gaseous products.

XRD patterns (Fig. 8) of the composite $\mathbf{2_{ox}}$ (oxidized at 1980 K) and $\mathbf{3_{ox}}$ (oxidized at 2190 K) indicated the presence of monoclinic zirconia inside the oxide layer. No peaks corresponding to silica-based phases were found, meaning silica-based oxides should be amorphous. XRD patterns obtained on the composite **2** oxidized at 1600 K or 1740 K were not different from the ones presented here: only monoclinic zirconia was observed. Especially no evidence of zircon at lower temperature was found. This means the surface composition involves only monoclinic zirconia and probably amorphous silica, despite what was expected from the phase diagram.

4. Conclusions

In summary, this study enables the understanding of the correlation between sintering and the oxidation mechanisms of ZrC_m/SiC_p composites, with different SiC amounts (0, 10 and 30 wt%), issued from the polymer derived ceramics route. The increase of the SiC content enhances the density and the Young's modulus of the composites elaborated thanks to SPS

process. Depending on the temperature and the SiC amount, different behaviors seem to be highlighted for the oxidation in ambient air. Indeed, the composition **3** (ZrC/SiC 30 wt%) indicates a good resistance to the oxidation up to 1800 K. Conversely, the composition **2** (ZrC/SiC 10 wt%) exhibits a better behavior at higher temperature (from 2000 K). Comparing with the monolithic ZrC, the SiC containing composites remain stable in oxidizing air atmosphere from 1600 to 2000 K. Furthermore, by modulating the SiC amount, the protection of the composite against the damaging effect of atmosphere can be improved on an adjusted temperature range. The stability and the respective volume fraction of generated oxides (ZrO_2 and SiO_2) seem to be the critical parameters which could affect the oxidation mechanism of composites.

Appendix A. Supporting information

Supplementary data associated with this article can be found in the online version at http://dx.doi.org/10.1016/j.ceramint.2013.08.105.

References

[1] M.J. Gasch, D.T. Ellerby, S.M. Johnson, Ultra high temperature ceramic composites, in: N.P. Bansal (Ed.), Handbook of Ceramic Composites, Kluwer Academic Publishers, New York, 2005, pp. 197–224.

[2] L. Kljajević, S. Nenadović, M. Gautam, T. Volkov-Husović, A. Devečerski, B. Matović, Spark plasma sintering of ZrC–SiC ceramics with $LiYO_2$ additive, Ceramics International 39 (2013) 5467–5476.

[3] B.P. Das, M. Panneerselvam, K.J. Rao, A novel microwave route for the preparation of ZrC–SiC composites, Journal of Solid State Chemistry 173 (2003) 196–202.

[4] Q. Li, S. Dong, P. He, H. Zhou, Z. Wang, J. Yang, B. Wu, J. Hu, Mechanical properties and microstructures of 2D Cf/ZrC–SiC composites using ZrC precursor and polycarbosilane, Ceramics International 38 (2012) 6041–6045.

[5] M. Baoxia, H. Wenbo, Thermal shock resistance of ZrC matrix ceramics, International Journal of Refractory Metals and Hard Materials 28 (2010) 187–190.

[6] N. Padmavathi, S. Kumari, V.V. Bhanu Prasad, J. Subrahmanyam, K.K. Ray, Processing of carbon-fiber reinforced (SiC+ZrC) mini-composites by soft-solution approach and their characterization, Ceramics International 35 (2009) 3447–3454.

[7] P.D. Bharat, M. Panneerselvam, K.J. Rao, A novel microwave route for the preparation of ZrC–SiC composites, Journal of Solid State Chemistry 173 (2003) 196–202.

[8] L. Houbu, Z. Litong, C. Laifei, W. Yiguang, Fabrication of 2D C/ZrC–SiC composite and its structural evolution under high-temperature treatment up to 1800 °C, Ceramics International 35 (2009) 2831–2836.

[9] P. Colombo, G. Mera, R. Riedel, G.D. Soraru, Polymer-derived ceramics: 40 years of research and innovation in advanced ceramics, Journal of the American Ceramic Society 93 (2010) 1805–1837.

[10] D. Pizon, R. Lucas, S. Chehaidi, S. Foucaud, A. Maître, From trimethylvinylsilane to ZrC-SiC hybrid materials, Journal of the European Ceramic Society 31 (2011) 2687–2690.

[11] D. Pizon, R. Lucas, S. Foucaud, A. Maître, ZrC–SiC Materials from the polymer-derived ceramics route, Advanced Engineering Materials 13 (2011) 599–603.

[12] F. Bouzat, S. Foucaud, Y. Leconte, A. Maître, R. Lucas, From click to ceramic: an efficient way to generate multielement Si/Zr/C clicked-polymer-derived ceramics (cPDC), Materials Letters 106 (2013) 337–340.

[13] H. Wang, C. Wang, X. Yao, D. Fang, Processing and mechanical properties of zirconium diboride-based ceramics prepared by spark plasma sintering, Journal of the American Ceramic Society 90 (2007) 1992–1997.

[14] R. Tu, H. Hirayama, T. Goto, Preparation of ZrB_2-SiC composites by arc melting and their properties, Journal of the Ceramic Societyof Japan 116 (2008) 431–435.

[15] Q. Qiang, Z. Xinghong, M. Songhe, H. Wenbo, H. Changqing, H. Jiecai, Reactive hot pressing and sintering characterization of ZrB_2–SiC–ZrC composites, Materials Science and Engineering, A 491 (2008) 117–123.

[16] A. Bellosi, F. Monteverde, D. Sciti, Fast densification of ultra-high-temperature ceramics by spark plasma sintering, Journal of Applied Ceramic Technology 3 (2006) 32–40.

[17] C. Potel, T. Chotard, J.-F. Belleval, M. Benzeggagh, Characterization of composite materials by ultrasonic methods: modelization and application to impact image, Composites Part B—Engineering 29B (1998) 159–169.

[18] L. Charpentier, M. Balat-Pichelin, F. Audubert, High temperature oxidation of SiC under helium with low-pressure oxygen-Part 1: Sintered α-SiC, Journal of the European Ceramic Society 30 (2010) 2653–2660.

[19] M. Balat-Pichelin, J.F. Robert, J.L. Sans, Emissivity measurements on carbon-carbon composites at high temperature under high vacuum, Applied Surface Science 253 (2006) 778–783.

[20] D. Alfano, L. Scatteia, S. Cantoni, M. Balat-Pichelin, Emissivity and catalycity measurements on SiC-coated carbon fibre reinforced silicon carbide composite, Journal of the European Ceramic Society 29 (2009) 2045–2051.

[21] M. Balat-Pichelin, J. Eck, J.L. Sans, Thermal radiative properties of carbon materials under high temperature and vacuum ultra-violet (VUV) radiation for the heat shield of the solar probe plus mission, Applied Surface Science 258 (2012) 2829–2835.

[22] E.K. Storms, The Refractory Carbides, Academic Press, New York-London, 1967.

[23] A.S. Shimada, A thermoanalytical study on the oxidation of ZrC and HfC powders with formation of carbon, Solid State Ionics 149 (2002) 319–326.

[24] B.F. Yudin, V.G. Borisov, Thermodynamic analysis of dissociative volatilization of silicon carbide, Refractories and Industrial Ceramics 8 (1967) 499–504.

[25] T. Narushima, T. Goto, T. Hirai, Y. Iguchi, High-temperature oxidation of silicon carbide and silicon nitride, Materials Transactions 38 (1997) 821–835.

[26] E.M. Levin, H.F. McMurdie, F.P. Hall, Phase Diagrams for Ceramists, The American Ceramic Society (, Columbus, 1956.